



A short-term *in situ* CO₂ enrichment experiment on Heron Island (GBR)

SUBJECT AREAS:
ECOLOGY
ATMOSPHERIC SCIENCE
CLIMATE CHANGE
EARTH SCIENCES

David I. Kline^{1*}, Lida Teneva², Kenneth Schneider³, Thomas Miard¹, Aaron Chai¹, Malcolm Marker⁴, Kent Headley⁵, Brad Opdyke⁶, Merinda Nash⁶, Matthew Valetich⁶, Jeremy K. Caves^{2,6}, Bayden D. Russell⁷, Sean D. Connell⁷, Bill J. Kirkwood⁵, Peter Brewer⁵, Edward Peltzer⁵, Jack Silverman⁸, Ken Caldeira³, Robert B. Dunbar², Jeffrey R. Koseff⁹, Stephen G. Monismith⁹, B. Greg Mitchell¹⁰, Sophie Dove¹ & Ove Hoegh-Guldberg¹

Received
29 March 2012

Accepted
4 May 2012

Published
21 May 2012

¹Global Change Institute and Coral Reef Ecosystems Laboratory, School of Biological Sciences, The University of Queensland, Brisbane, Australia, and the ARC Centre of Excellence for Coral Reef Studies, ²Environmental Earth System Science, Stanford University, Stanford, California, USA, ³Carnegie Institution, Department of Global Ecology, Stanford, CA, USA, ⁴Faculty of Engineering, Architecture and Information Technology, The University of Queensland, Australia, ⁵Monterey Bay Aquarium Research Institute, Monterey, California, USA, ⁶Australian National University, Canberra, Australia, ⁷University of Adelaide, School of Earth and Environmental Sciences, Australia, ⁸Israel Oceanographic & Limnological Research Ltd., Haifa, Israel, ⁹Civil and Environmental Engineering, Stanford University, Stanford, California, USA, ¹⁰Scripps Institution of Oceanography, Integrative Oceanography Division, University of California, San Diego, USA.

Correspondence and requests for materials should be addressed to D.I.K. (dkline@ucsd.edu)

* Current address: Scripps Institution of Oceanography, Integrative Oceanography Division, University of California, San Diego, 9500 Gilman Drive, MC 0218, La Jolla, CA, 92093-0218.

Ocean acidification poses multiple challenges for coral reefs on molecular to ecological scales, yet previous experimental studies of the impact of projected CO₂ concentrations have mostly been done in aquarium systems with corals removed from their natural ecosystem and placed under artificial light and seawater conditions. The Coral-Proto Free Ocean Carbon Enrichment System (CP-FOCE) uses a network of sensors to monitor conditions within each flume and maintain experimental pH as an offset from environmental pH using feedback control on the injection of low pH seawater. Carbonate chemistry conditions maintained in the -0.06 and -0.22 pH offset treatments were significantly different than environmental conditions. The results from this short-term experiment suggest that the CP-FOCE is an important new experimental system to study *in situ* impacts of ocean acidification on coral reef ecosystems.

Atmospheric CO₂ levels are rising rapidly due to increasing fossil fuel combustion, deforestation, and construction^{1,2}. The current CO₂ concentration of 389 ppm is the highest seen during the last 800,000 years, if not since the middle Pliocene (~3 million years ago), with a rate of increase ~2 orders of magnitude faster than during any time within the last 300 million years, with the possible exception of major mass-extinction events^{3,4}. The world's oceans have absorbed over 25% of the CO₂ emitted to the atmosphere since the beginning of the industrial revolution^{2,5} resulting in a decline in oceanic pH, termed ocean acidification (OA)^{6,7}. Since pre-industrial times the ocean's pH has declined by ~0.1 pH units⁶, representing a ~30% increase in hydrogen ion concentrations, and a rate of decline ~2 orders of magnitude faster than during glacial-interglacial transitions^{8,9}. Oceanic pH in the year 2100 has been predicted to decline by up to an additional 0.2 to 0.5 pH units under the United Nations International Panel on Climate Change (IPCC) scenarios for CO₂ emissions^{9,10}, levels more extreme than those seen in the last 40 million years⁸. Coral reefs are likely to be particularly vulnerable to ocean acidification; as reductions in calcification rates may influence the delicate balance between growth rates and erosional forces.

There is abundant evidence from laboratory experiments that OA causes reduced calcification in marine organisms¹¹⁻¹³, however, the physiological impacts are often complex and life-stage dependent^{14,15}. OA is likely to have synergistic impacts on the resilience of coral reefs to other disturbances including global warming (i.e. bleaching and disease events), local human stressors (e.g. declining water quality, over-fishing), and increased storm frequency and intensity^{16,17}. It has also been suggested that the combined effects of hypoxia and OA may lead to the expansion of marine dead zones as increasing CO₂ concentrations further lowers the respiration index¹⁸. However, as most coral reefs are in the mixed layer and presumably in equilibrium with the atmosphere, hypoxia will likely not be a major factor. Yet, for studies below the mixed layer or in regions where the upwelling of low oxygen water onto the continental shelf is common or predicted as possible in the near future, the non-linear effects of combined hypoxia and hypercapnia should be considered. In addition, coral coring studies have



revealed a 20% decline in coral calcification rates over the last 20 years across the Great Barrier Reef, which is consistent with the impacts of increasing sea temperature and possibly ocean acidification^{19,20}. It has even been predicted that one third of coral species face extinction associated with global warming, OA and local stressors²¹.

Marine ecosystems have been shown to have large regional and diel variability in pH²², and recently variability in pCO₂ and pH within reef systems has been demonstrated. pCO₂ levels measured from the Lady Elliott Island reef flat, Southern Great Barrier Reef, showed variations as extreme as 200 ppm–1300 ppm in a single diel cycle²³. In Ningaloo reef (Western Australia) and Lizard and Magnetic Islands (GBR) pH fluctuations of up to 0.42 pH units were measured, with the variations dependent on sampling locality rather than diel cycles²⁴. Similarly, diel pH changes as high as 0.75 have been recorded in the Heron Island reef lagoon²⁵. In Palmyra, Northern Line Islands a pH range of 0.253 was measured on the reef terrace and 0.121 on the fore reef, while a fringing reef in Moorea, French Polynesia had a pH range of 0.101 and both locations showed clear diel cycles in pH²². Incorporating regional and diel variability in pH into OA experiments will be critical for better understanding the future impacts of OA on marine ecosystems²².

Studies of natural systems with high CO₂ levels such as vent sites and upwelling areas are beginning to provide critical data about the long-term impacts of ocean acidification on organisms, communities and ecosystems^{26–28}. Studies from CO₂ vent sites reveal a decline in reef rugosity, diversity, and the prevalence of calcareous organisms with declining pH levels^{26,28,29}. Similarly, coral reefs near coastal margins with upwelling of deep lower pH waters have revealed that coral reefs in a high CO₂ world will likely be poorly cemented³⁰. Furthermore, biogeography studies reveal that cold-water corals^{31,32} and scleractinian corals³³ tend to grow in areas with higher aragonite saturation states ($\Omega_{\text{arag}} > 1$ and > 3.5 respectively). Additionally, *in situ* studies conducted with the Submersible Habitat for Analyzing Reef Quality (SHARQ), a clear incubation tent to monitor *in situ* calcification rates without CO₂ manipulation, revealed that a reef flat in Hawaii begins dissolving between 467–1003 μatm of CO₂ depending on the substrate type^{34,35}. Further support for these measurements was provided by a long coral reef metabolism record from the Gulf of Eilat that demonstrated a positive relation between calcification and Ω_{arag} , temperature and nutrients³⁶. This empirical relation was applied to reefs globally using model results of Ω_{arag} and sea surface temperature³⁷ indicating that reef calcification rates will decline in the future and will eventually start to dissolve when atmospheric CO₂ levels reach twice their preindustrial levels (560 ppm). However, it has been suggested that coral acclimation may be a mechanism to reduce OA impacts on coral calcification and research into this topic is ongoing^{38–40}.

While important insights have been gained from natural *in situ* experiments, these studies have not allowed for experimental control over treatment conditions. In these studies, organisms are often exposed to pH levels that are more extreme and variable than those that are predicted to occur in the next century. Furthermore, confounding environmental factors often make the results difficult to interpret⁴¹. Additionally, these often extreme *in situ* conditions frequently occur as a pulse, with brief extreme conditions, rather than as a chronic stress as would occur if pH were delta offset from controls as will occur with OA. *In situ* carbon dioxide perturbation experiments allow for greater replication and better control over treatment conditions. In 2007, the Monterey Bay Aquarium Research Institute (MBARI) developed the FOCE (Free Ocean Carbon Enrichment) experimental system, which allowed for highly controlled semi-enclosed experiments in the deep sea within a 1 × 1 × 0.5 m enclosure within a flume^{41,42}. We modified the MBARI FOCE system for application to the challenging conditions found on coral reefs including warm temperatures, high flow rates, high UV, and high wave energy⁴³. The Coral Proto – Free Ocean Carbon Enrichment system

(CP-FOCE) was developed to test the impact of ocean acidification on coral reef organisms in as natural a reef setting as possible. *In situ* experiments make it possible to study how organisms and ecosystems respond to lowered pH and Ω_{arag} with natural conditions including the associated reef biodiversity, ecosystem interaction, ambient seawater chemistry, natural sediment communities, as well as diel and seasonal changes in environmental conditions⁴¹. The CP-FOCE provides an important experimental platform to study the complex, interactive impacts of ocean acidification on coral reef organisms. It was designed to produce predicted future pH conditions as an offset from environmental conditions within discrete limits *in situ*, to test the effects of future conditions on the coral reef community. Here we present results from a short-term deployment on the Heron Island reef flat with three pH levels and experimental flumes containing key ecological elements of the reef community, corals (*Acropora millepora*), crustose coralline algae (CCA, *Porolithon onkodes*), and reef sediments.

Results

Carbonate Chemistry Measurements. Carbonate chemistry measurements taken in the three CP-FOCE flumes and the environment reveal typical diel variability in all of the measured parameters (Fig. 1). Dissolved Inorganic Carbon (DIC) in all flumes decreased during the day and increased during the night. The difference between the −0.06 pH treatment and the environment had consistently higher DIC values than the control minus the environment, and the difference between −0.22 pH treatment and the environment was consistently higher than the −0.06 pH and the control treatments, except during the low tide slack water periods when there was slower water movement. When the DIC measurements were compared across a four-day period (Fig. 2A), the average values as offset from the environment were 3.98 ± 19.39 ($\pm\text{SD}$) for the controls, 48.68 ± 56.41 for the −0.06 pH treatment and 101.04 ± 53.64 for the −0.22 treatment. The −0.06 pH treatment had significantly greater offsets compared to the control offsets with respect to the ambient DIC (Table 1, $n=23$, $p=0.00082$, $df=44$, $F=12.91$, Single Factor ANOVA). The −0.22 pH treatment produced even greater DIC excursions from ambient conditions compared to the control (Table 1, $n=23$, $p=2.4 \times 10^{-10}$, $df=44$, $F=66.61$, Single Factor ANOVA). Additionally, the DIC offset was significantly higher in the −0.22 pH treatment than in the −0.06 pH treatment (Table 1, $n=23$, $p=0.0024$, $df=44$, $F=10.41$, Single Factor ANOVA).

Total alkalinity (A_T) measurements were almost identical across the experimental period except for some variability during slack low tides (Fig. 1B,D). There was no significant difference in A_T values across the 3 CP-FOCE flumes during the course of the four-day experiment ($n=23$, $p=0.923$, $df=66$, $F=0.08$, Single Factor ANOVA).

The pH measurements were almost identical between the environment and the control treatments, except during the low tide slack water periods. The pH measurements in the environment showed a diel variation, with a maximum pH during the day of over 8.4 (at around 16:30 local time) and a minimum pH of 8.0 at night (around 03:30 local time; Fig. 1C). The control CP-FOCE flume also showed extreme diel cycles with a maximum pH of over 8.3 during the day and a minimum pH below 7.9 at night, values very similar to those measured by Santos et al. (2011) on the same reef flat the week before this experiment was conducted⁴⁴. The pH in the −0.06 pH unit treatment was lower than the control treatment by an average value of 0.055 ± 0.11 ($\pm\text{SD}$). Similarly, the pH in the −0.22 pH treatment was consistently lower than the −0.06 pH by an average of 0.17 ± 0.18 and from the control treatments by an average of 0.23 ± 0.15 . The recorded pH offsets from the environment in the −0.06 pH treatment was significantly lower than the control (Table 1, $n=23$, $p=0.014$, $df=44$, $F=6.55$, Single Factor ANOVA) as were those in the −0.22 pH treatment (Table 1, $n=23$,

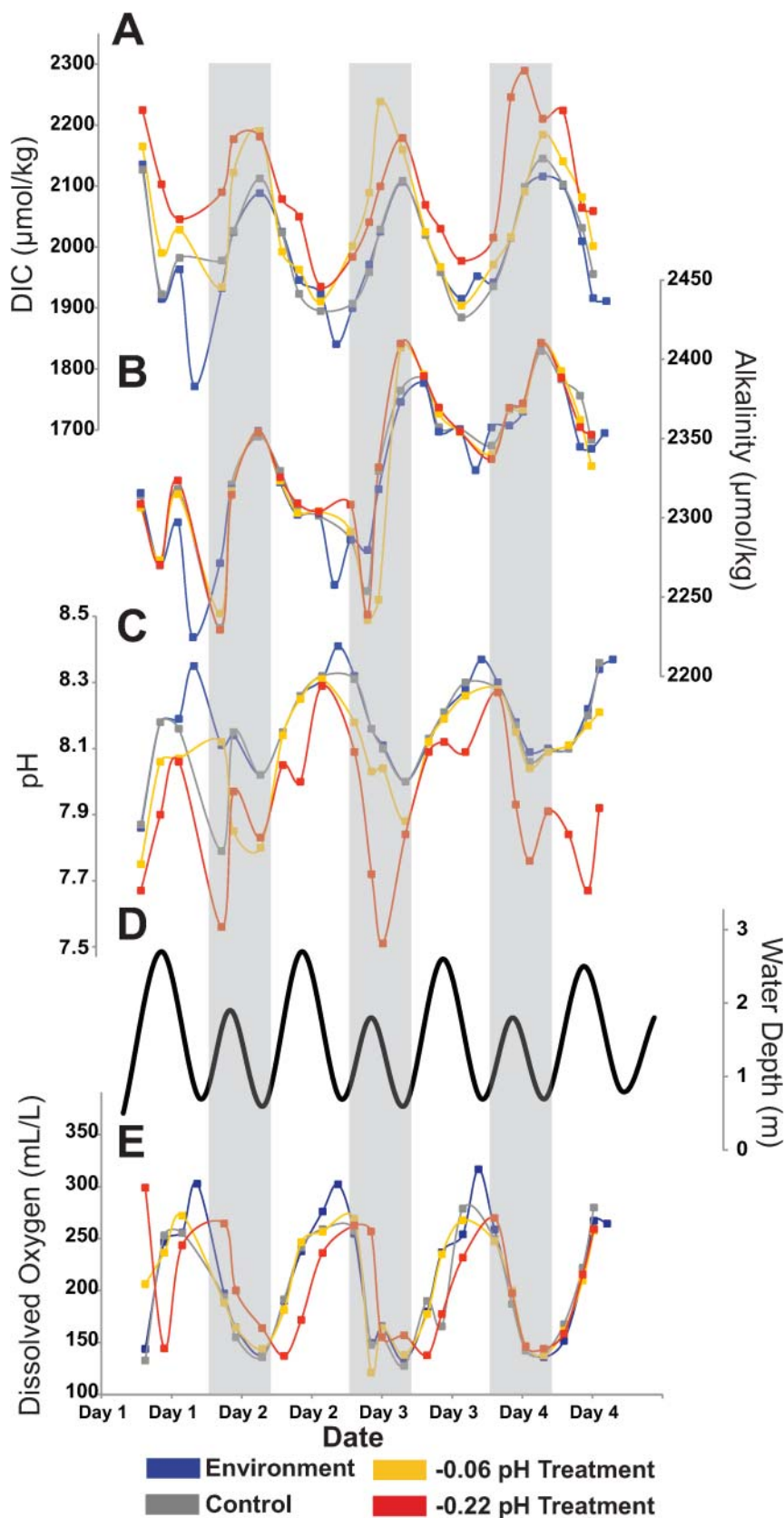


Figure 1 | Diel fluctuations in seawater chemistry in the environment and the three CP-FOCE flumes for the short-term experiment on the Heron Island reef flat. Discrete carbonate chemistry measurements (DIC, ALK, pH, O₂) were made every 3–6 hours throughout the experiment. The system was able to manipulate pH at environmental flow rates up to $0.1 \text{ m} \cdot \text{s}^{-1}$, which could explain why pH and DIC control was not as controlled during transitions from low to high tides and vice versa as these were periods of maximum flow rates. Grey shading indicates night time periods with no light.

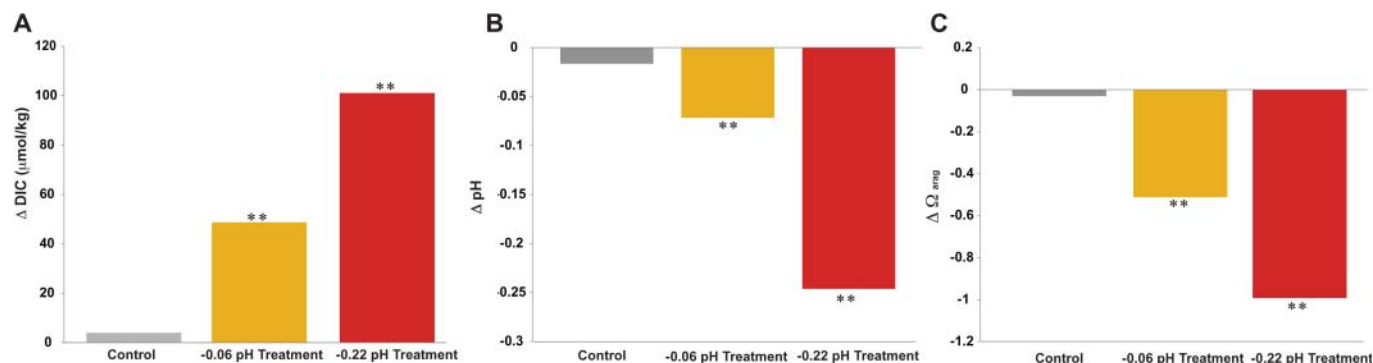


Figure 2 | Changes in carbonate chemistry measurements in the 3 CP-FOCE flumes. Average offsets from ambient carbonate chemistry, recorded in the control, -0.06 and -0.22 treatment flumes including A) DIC and B) pH and C) calculated Ω_{arag} in the three CP-FOCE flumes throughout the course of the 4 day experiment. ** Denote that the treatments were significantly different from the controls and each other at $p < 0.05$.

$p = 2.4 \times 10^{-7}$, $df = 42$, $F = 39.72$, Single Factor ANOVA). Additionally, the -0.22 pH treatment had significantly lower pH than the -0.06 pH treatment (Table 1, Fig. 2B, $n = 23$, $p = 5.6 \times 10^{-5}$, $df = 44$, $F = 20.47$, Single Factor ANOVA).

Dissolved oxygen measurements were similar during the control and the environment except during low tide period during the day when they were higher in the environment (Fig. 1E). The dissolved oxygen measured in the -0.06 pH treatment was consistently similar to the control dissolved oxygen except during low tide during the day when it was higher in the -0.06 treatment. The dissolved oxygen measurements in the -0.22 treatments were consistently lower than the other treatments during the day and higher at night although these trends became less pronounced from the first to the fourth day of the experiment.

The average calculated value of Ω_{arag} in the control flume was 3.76 ± 0.70 (\pm SD), in the -0.06 flume it was 3.28 ± 0.98 , and in the -0.22 flume it was 2.80 ± 0.88 . Thus, the average decline in the Ω_{arag} for the -0.06 pH and the -0.22 pH treatments relative to the control were 0.48 ± 0.64 and 0.96 ± 0.50 , respectively (Fig. 2C). Ω_{arag} values in the -0.06 pH and -0.22 pH treatments were significantly lower than the control (Table 1, $n = 23$, $p = 0.0029$, $df = 44$, $F = 10.59$; and $n = 23$, $p = 4.2 \times 10^{-9}$, $df = 44$, $F = 53.22$; respectively) as well as significantly different from each other (Table 1, $n = 23$, $p = 0.012$, $df = 44$, $F = 6.90$). The change in Ω_{arag} between the experimental and control flumes indicates that the CO_2 enrichment in the CP-FOCE was effective.

Sediment and coralline algae dissolution and mineralogy. Surface sediment samples were taken from each of the flumes and the environment at the end of the experiment to assess if any pH related change in the amount of Mg-calcite present or the average mol % MgCO_3 of the Mg-calcite⁴⁵ occurred (Fig. 3). These samples were collected within meters of each other and present a range

of sediment mineralogy with average mol % MgCO_3 varying from 15.1–15.7 mol %, quantity of aragonite from 36–41%, and the calcite Mg-calcite group 64–59%. There was no significant difference between the control and environmental mol % MgCO_3 or Mg-calcite quantity, compared to the -0.06 pH or -0.22 pH treatments at the end of the experimental period. However, approximately 20% of the Mg-calcite quantity would need to dissolve for there to be a measurable change in sediment Mg-calcite quantity that could be attributable to the treatments.

CCA samples showed weight losses (dissolution) of 1.22 %, 1.76 % and 2.12 % for the control, -0.06 pH and -0.22 pH treatments, respectively (Table 2, Fig. 4). For the control and -0.1 pH treatments the % aragonite was lower in the CCA samples with least weight loss, but there was only a weak correlation for the -0.22 pH treatment (Fig. 4A). Weight loss was lower in CCA samples with higher mole % MgCO_3 as measured by ICP (Fig. 4B).

Discussion

The CP-FOCE as an *in situ* system avoids many of the problems associated with tank or mesocosm experiments such as unnatural light, isolation from key local hydrodynamics, controls on food energetics, disturbed microbial populations, lack of sediment and associated animal communities. Importantly, it allows for well-controlled *in situ* OA experiments with realistic future pH maintained as an offset from environmental conditions, as opposed to being limited by the often extreme pH variations often associated with natural experiments such as at CO_2 vents^{26,28}.

The carbonate chemistry measurements from the environment reveal diel variations in DIC, pH, alkalinity, and dissolved oxygen that roughly followed the light intensity/dark cycle with the tidal cycle superimposed on it (Fig. 1). The carbonate chemistry clearly had an association with the tidal cycles, but the metabolic signal is likely stronger and controls the diel swings in carbon chemistry, which is exaggerated at low tide when the seawater is stagnant. Daytime decline in DIC and increase in pH and O_2 (Fig. 1) were the result of net photosynthesis by the reef community. At night, the trend was reversed as respiration by reef organisms increased the DIC and decreased the pH and O_2 . A_T maxima near sunrise are attributed to low precipitation and/or dissolution of CaCO_3 during the night and A_T minima near sunset would be due to the cumulative effect of daytime calcification. While our sampling resolution does not allow for an estimation of rates of change in DIC, pH, and O_2 on an hourly basis, the data suggest that the fastest rates of change occur shortly after sunrise and shortly after sunset. This is probably caused by the physiological shifts on the reef from day to night metabolism. A longer dataset will be necessary to decouple the contributions of light-driven reef metabolism and tidal hydrodynamics on the trends in the carbon system parameters, but in shallow reef flats due to a

Table 1 | P-values for ANOVA on carbonate chemistry measurements from the 3 CP-FOCE flumes. All treatments were significantly different from each other and the control flume for pH, Dissolved Inorganic Carbon (DIC) and Aragonite saturation state (Ω_{arag})

| | Control | -0.06 pH Treatment | -0.22 pH Treatment |
|------------------------|------------|----------------------|-----------------------|
| pH | Control | 0.014 | 2.4×10^{-7} |
| | -0.06 pH | | 4.5×10^{-5} |
| DIC | Control | 0.00082 | 2.4×10^{-10} |
| | -0.06 pH | | 0.0024 |
| Ω_{arag} | Control | 0.0029 | 4.2×10^{-9} |
| | -0.06 pH | | 0.012 |

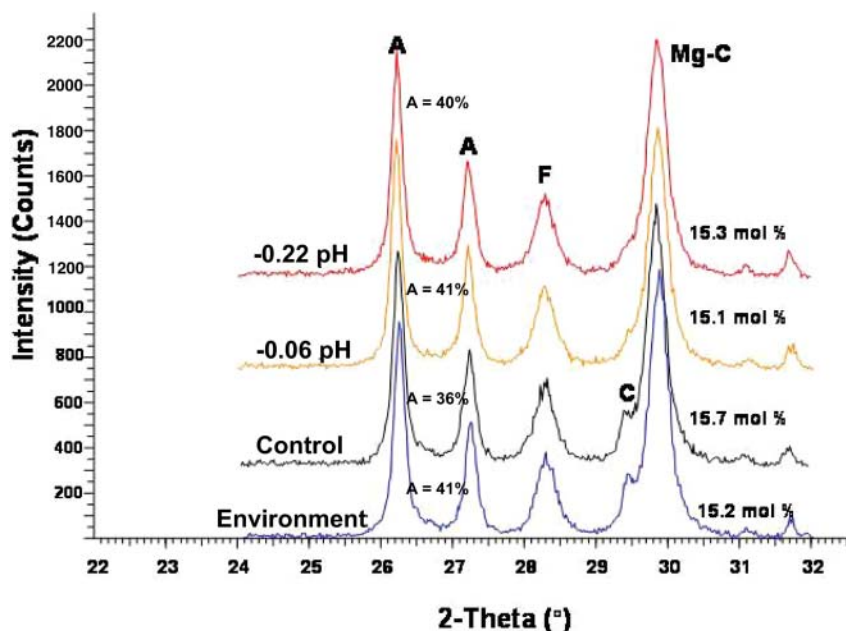


Figure 3 | X-Ray Diffraction (XRD) patterns for surface sediment samples taken after 4 days of experimental treatment. Scans for control, -0.06 pH and -0.22 pH treatments have been stacked for ease of viewing and their scale is the same as for the environment scan. In this figure: A = aragonite peaks with % aragonite, F = fluorite standard, C = calcite, Mg-C = Mg calcite with mole % Mg calcite.

smaller water volume and slower exchange with the water beyond the reef, the biological signal of reef community metabolism tends to be the dominant modulator of carbon and oxygen budgets on diurnal and seasonal time-scales.

The data presented here clearly demonstrate that the CP-FOCE approach successfully produced and maintained experimental conditions in the treatment flumes closely and consistently tracking the environmental conditions with an offset in the DIC and pH levels with the -0.06 pH treatment consistently higher than the control, and the -0.22 pH treatment consistently higher than the -0.06 pH treatment (Fig. 2). The demonstration from this prototype system has significant implications, as it indicates that similar manipulative experiments can be conducted on other reefs and in other coastal ecosystems with valuable scientific outcomes.

XRD results showed that most CCA samples (16 of 19) had aragonite present, six displayed asymmetrical Mg-calcite curves which represented the presence of dolomite ($\text{Ca}_{0.5}\text{Mg}_{0.5}\text{CO}_3$) and magnesite (MgCO_3) within the CCA crust⁴⁶ and seven displayed asymmetry potentially indicative of dolomite (Table 2). There are trends of

increasing weight loss with increasing aragonite across all treatments (Figure 4A), correlation is strong for control and -0.06 pH with a R^2 of 0.58 ($n = 8$) and 0.89 ($n=6$) respectively, however poor for -0.22 pH 0.08 with a R^2 of ($n=8$). There was no clear trend with mol % MgCO_3 and dissolution, however, 3 of the 4 highest mol % were in the lower weight loss grouping. Notably, samples with the smallest weight loss typically had very asymmetrical XRD Mg-calcite curves. The ICP-AES bulk magnesium mol % MgCO_3 shows a clear trend. The two CCA samples with the lowest bulk magnesium [22.61 (control) and 15.64 (-0.22 pH) mol % MgCO_3] lost more than 7 times the weight than those with higher magnesium [27.01 (control) and 23.8 (-0.22 pH) mol % MgCO_3] (Figure 4B). Changes in mineralogy from a weight loss of 2–3% are likely below the detection level of the XRD method and could not account for the 8% difference in ICP in the -0.22 pH treatment. Magnesium enriched CCAs (Fig 4B) demonstrated dolomite ($\text{Mg}_{0.50}\text{CaCO}_3$) and magnesite (MgCO_3) features in XRD. These results suggest that magnesium enrichment by dolomite and magnesite lead to reduced dissolution relative to corallines with magnesium enriched phases. Although there was not

Table 2 | Summary of mineralogy results for the crustose coralline algae samples in the 3 CP-FOCE flumes. Samples with weight gains were excluded from analysis (control $n=2$, -0.06 pH $n=4$, -0.22 pH $n=2$) as the samples were not living and weight gain is assumed to be from sediment grains lodging on the sample. Replicate 10 day experiments in flow through aquarium tanks without sediment and using the same sample preparation did not have any weight gain. Mol % MgCO_3 measurement precision ± 0.3 mol % MgCO_3 . * indicates a sample with aberrantly high % aragonite that was excluded from the linear regression in Fig. 5A

| Control | weight loss % | mol % MgCO_3 | arag. % | -0.06 pH | weight loss % | mol % MgCO_3 | arag. % | -0.22 pH | weight loss % | mol % MgCO_3 | arag. % |
|----------------|---------------|-----------------------|---------|----------------|---------------|-----------------------|---------|----------------|---------------|-----------------------|---------|
| | 0.16 | 17.6 | 0.0 | | 0.07 | 17.6 | 2.6 | | 0.58 | 16.1 | 6.8 |
| | 2.09 | 17.3 | 5.6 | | 1.13 | 16.6 | 46.6* | | 3.04 | 17.3 | 14.8 |
| | 1.03 | 17.4 | 0.0 | | 0.16 | 16.5 | 4.7 | | 6.48 | 16.1 | 4.0 |
| | 0.27 | 16.3 | 2.9 | | 0.59 | 17.6 | 4.5 | | 1.32 | 16.7 | 0.0 |
| | 1.07 | 16.3 | 4.6 | | 2.18 | 16.6 | 5.5 | | 0.59 | 16.9 | 3.7 |
| | 0.36 | 16.4 | 3.3 | | 6.45 | 17.7 | 8.8 | | 1.46 | 16.8 | 2.4 |
| | 0.52 | 16.9 | 1.5 | | | | | | 3.11 | 16.3 | 9.7 |
| | 4.21 | 17.2 | 7.0 | | | | | | 0.41 | 17.2 | 1.9 |
| Avg | 1.21 | 16.9 | 3.1 | Avg | 1.76 | 17.1 | 12.1 | Avg. | 2.12 | 16.7 | 5.6 |
| st.dev. | 1.36 | 0.54 | 2.55 | st.dev. | 2.42 | 0.59 | 16.99 | st.dev. | 2.05 | 0.46 | 5.18 |

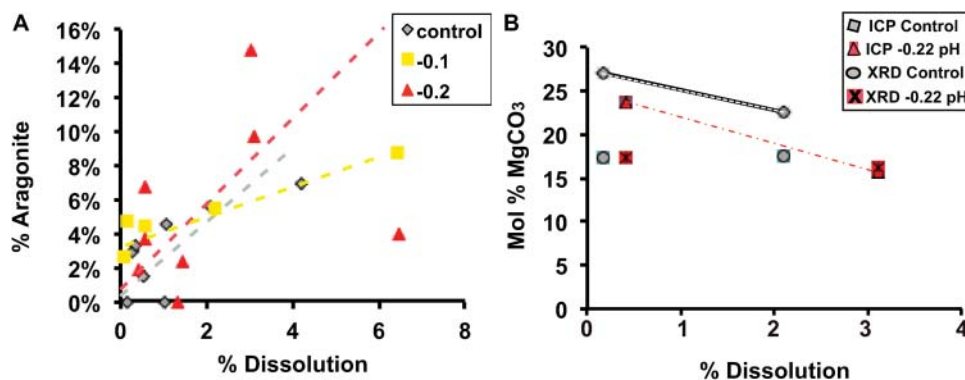


Figure 4 | Crustose coralline algae (CCA) dissolution rates and mineralogy. A) CCA aragonite percentage with linear least squares correlation lines fitted using a model-2 geometric means technique⁵⁹ (control $R^2 = 0.58$, -0.06 pH treatment $R^2 = 0.89$, -0.22 pH treatment $R^2 = 0.08$). There is increasing weight loss with increasing % aragonite across all treatments however correlation is poor for the -0.22 pH treatment. B) mol % $MgCO_3$ determined by x-ray diffraction (XRD) and by inductively coupled plasma atomic emission spectroscopy (ICP-AES) for four CCA dissolution samples. XRD mol % $MgCO_3$ is determined by measuring the shift in the Mg-calcite peak relative to the calcite peak position. XRD mol % $MgCO_3$ determines the Mg-calcite phase and allows for identification of other carbonate minerals present whereas ICP-AES measures the average mol % $MgCO_3$ across all Mg-containing minerals. It is commonly assumed that CCA are high Mg-calcite^{16,60} and that the more Mg present the more susceptible the carbonate is to dissolution³⁷. Contrary to this presumption, within the control and the -0.22 treatment the CCA samples with lower % Mg (measured with ICP-AES) had the higher weight loss (by a factor of 7). Detailed mineralogical analyses on the Mg-enriched CCA revealed that as well as Mg-calcite there is also dolomite (50 mol % $MgCO_3$) and magnesite (100 mol % $MgCO_3$) present⁴⁶. Three samples also had aragonite present (5.6, 6.8 and 14.8 % respectively). These results suggest that for these CCA it is not the Mg-calcite mol % $MgCO_3$ that exerts the greatest control on dissolution rates but the presence of dolomite and magnesite with aragonite adding a confounding factor.

sufficient replication in the bulk-magnesium samples for statistical tests, these preliminary data warrant further investigation as they are clearly in contrast with existing theories that predict increased dissolution with increasing magnesium content⁴⁵ and support the proposition that magnesium content is only a minor factor in biogenic Mg-calcite solubility¹⁷. The discovery of aragonite, dolomite and magnesite in the CCAs together with these results will necessarily require a reconsideration of applicability of the $\Omega_{Mg-calcite}$ for predicting impacts of OA on CCAs.

This is the first *in situ* study to demonstrate the ability to simulate ocean acidification conditions in a shallow coastal ocean environment. Our results show that it can accurately change the carbonate chemistry of ambient seawater, simulating future predicted conditions of ocean acidification. This is the first study to document the predicted pH conditions simulated as an offset from the pH conditions that change naturally throughout the diel cycle on the reef flat especially at low tide where a relation between photosynthesis, respiration, calcification and $CaCO_3$ dissolution control the ambient pH. This capability is extremely valuable and highlights the importance of running experiments as an offset from environmental conditions rather than as a constant pH.

The simulation of future pH changes, however is not linear because changes in DIC associated with respiration, photosynthesis and OA will lead to non-linear changes in pCO_2 and pH influencing diel carbonate chemistry fluctuations⁴⁷. The CP-FOCE could be modified to control for other carbon system parameters such as Ω_{arag} , but pH is a convenient control variable from an engineering perspective as it can be measured directly with an electrode, while controlling for other parameters would require either making assumptions about or measurements of other carbon system parameters.

Both monitoring large natural diel variations in pH as well as simulating large diel pH variations with an offset towards more acidic conditions can provide valuable insight into ocean acidification sensitivity of various reef organisms and environments. As these reef flat communities regularly experience pH changes equivalent to conditions ranging from preindustrial levels (280 ppm) to those predicted for 2100 (600–1000 ppm) in one diel cycle, perhaps they are less vulnerable to ocean acidification than other reef sub-environments.

Reef flat communities may be particularly acclimated to large diel fluctuations in pH and thus be more tolerant to future ocean acidification when compared to other reef sub-environments. Alternatively, future predicted ocean acidification associated pH offsets may lower nighttime reef flat pH below a critical threshold that could cause increased dissolution of $CaCO_3$ as indicated by the finding of Tribollet *et al.* (2009)⁴⁸. Clearly, more CP-FOCE type experiments in different reef sub-environments are needed to further elucidate the relative vulnerability or resilience of different parts of the reef. Systems such as the CP-FOCE are likely to provide important insights into the factors that confer resilience or vulnerability of various reef sub-environments (lagoons, reef flats, reef fronts, etc) to future pH decline. The experimental approach can be deployed in a variety of coral reef, kelp forest, and estuarine settings and can offer insights into species-to-ecosystem scale biological impacts of ocean acidification.

Methods

The CP-FOCE uses replicate experimental flumes to enclose sections of the reef and dose them with CO_2 enriched seawater using peristaltic pumps with computer controlled feedback dosing (Fig. 5)⁵¹. Each flume is connected to a waterproof computer pod (National Instruments, CompacRIO, TX, USA) for pH control and to log its instruments including MBARI digital pH sensors (Nido Instruments, CA, USA), acoustic velocimeters (Nortek AS, Vectrinos, Rud, Norway), and a Conductivity, Temperature, Depth instrument (SBE-16plusV2 SEACAT, Sea-Bird Electronics, WA, USA). In addition, an identical set of sensors was deployed in ambient conditions on the reef flat to monitor environmental conditions and to determine a baseline for pH offsets (Fig. 5A).

pH Dosing. Seawater from the Heron Island Research Station aquarium system is pumped from the reef flat near the experiment and is treated on shore with CO_2 in a 1000 L sealed tank to reduce its pH to around 5.0. The water then passes through $\frac{1}{2}$ " polyethylene white plastic tubing to the 6 peristaltic pumps (2 per flume, Watson-Marlow Inc., 520 FDM, Wilmington, MA, USA) that are mounted in a waterproof housing on the instrumentation float. A parallel tank with seawater without CO_2 addition is also connected to the control flume. Feedback control of the pH is provided by the pH, temperature, and current velocity and speed measurements to determine whether the forward or reverse peristaltic pump should be activated and at what rate (Fig. 5E). The pH treatments are produced as an offset from the environment pH levels in order to have treatments reflect the diel variation in reef flat pH. The difference from the environment pH and the experimental offset determines the flume pH set point that is compared to the pH measured in the flume. This produces an error value, which is processed by a simple Proportional and Integral (PI) control algorithm. The PI algorithm parameters are tuned to optimally operate over



the measured range of flow rates, and produces a demand signal that is converted to pulse width modulation (PWM) to control the power going to the dosing pump motors. The flow direction and speed is determined by the current measurements and the direction of the flow is used to determine which dosing pump motor is turned on so that the low pH water is added in the direction of the ambient flow (Fig. 5E). pH

dosing did not work effectively at flow speeds above $0.1 \text{ m} \times \text{s}^{-1}$ in the chambers because of the pumping rates required to sufficiently lower the pH within the flumes at these high flow rates. The cross-sectional area of each flume is 0.0625 m^2 , and for a 0.3 pH offset the approximate required flow rate for the pH 5.0 water addition at a chamber flow speed of $0.1 \text{ m} \times \text{s}^{-1}$ would be approximately $1.5 \text{ L} \times \text{s}^{-1}$ and for a

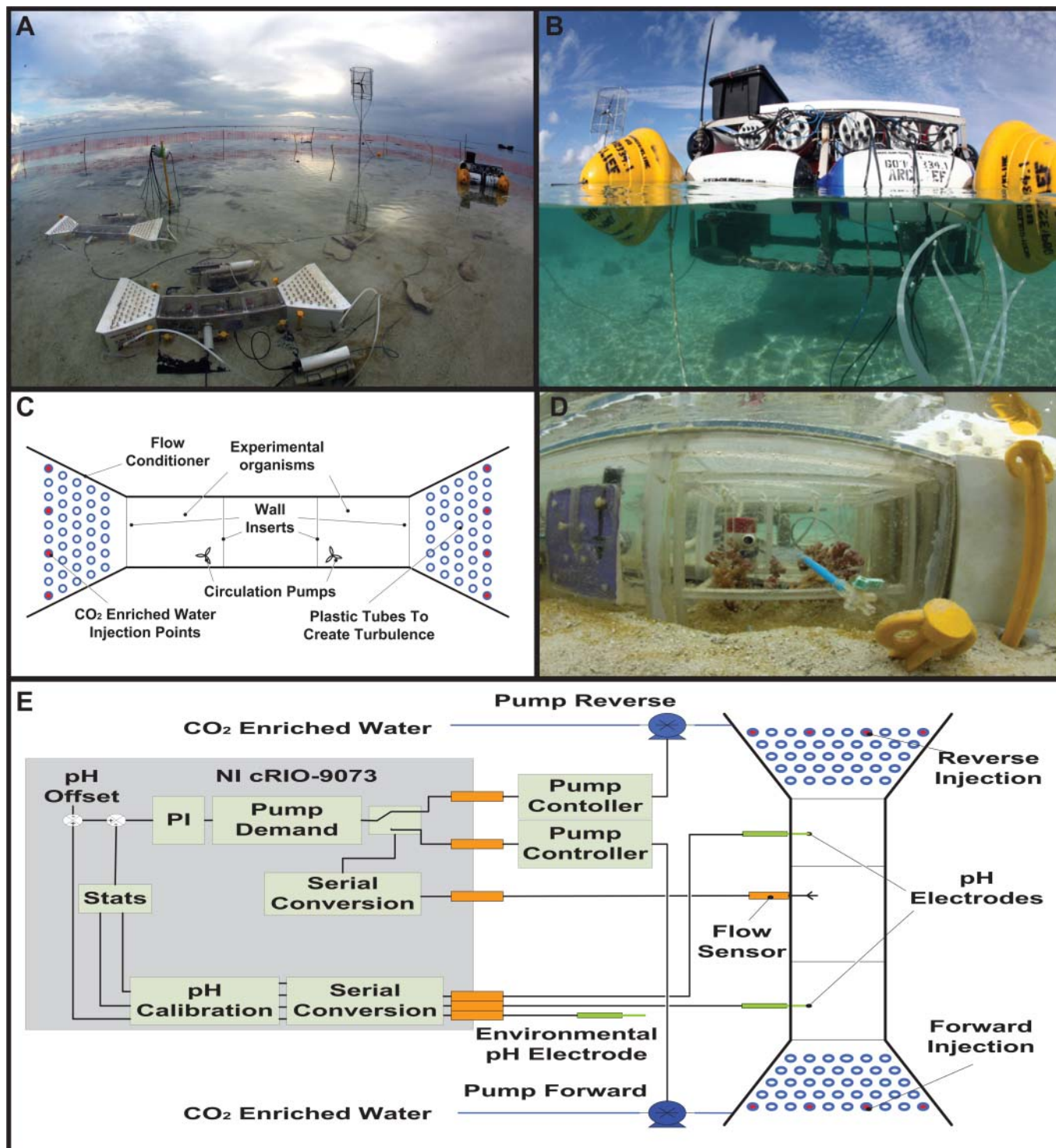


Figure 5 | Photographs and schematics of the CP-FOCE as deployed on the Heron island reef flat in December 2009. A) Shows a wide view of the experimental system including the 3 CP-FOCE flumes and the wind generator. B) Photograph of the experimental float that has the 4, 12 V deep cycle batteries as ballast, and contains all of the control computers, peristaltic pumps, the solar panel, and the radio antennae to transmit the data real-time back to the laboratory. C) Schematic of a CP-FOCE flume showing the 3 experimental sections and the flow conditioners with CO_2 enriched seawater injection sites. D) Photograph of a section of a CP-FOCE flume containing a rack with *Acropora millepora* corals and the pump that is turned on when the doors are closed to provide water movement. E) Schematic of the feed-back control between the pH sensors, flow sensor and the National Instrument control computers which decide which peristaltic pump to turn on and at what rate for the dosing.



−0.15 pH offset it would be $0.75 \text{ L} \times \text{s}^{-1}$, while the max pumping rates of the 520 FDM Watson-Marlow pumps was approximately $1.5 \text{ L} \times \text{s}^{-1}$. Therefore, flow rates above $0.1 \text{ m} \times \text{s}^{-1}$ would make pH control challenging. The system could be modified in the future to accommodate higher flow rates by having a larger capacity CO_2 delivery system, having greater residence time or by using a flow reduction system that reduces flow speeds within the flumes in a feed-back control loop with the flow sensors.

A CP-FOCE flume consists of forward and rear flow conditioners on either end of an experimental flume. The flume is placed parallel to the direction of flow of tidal movements on the reef flat and attached with sand stakes. The flume is semi open at both ends to allow bi-directional tidal flow through the flume (Fig. 5C). At either end of the experimental flumes flow conditioners are attached to minimize turbulence and eddies in order to simplify pH control and to provide passive mixing of the CO_2 enriched seawater (Fig. 5C). Four of the pvc tubes in the flow conditioners furthest from the flume have small holes along their entire length in which the low pH water is pumped to ensure that is released evenly along the entire width and height of the conditioner. The flow conditioners are based on a design that has been previously used in flume studies³⁹ and are painted white to minimize heating and algal growth.

Flume Design. The experimental flumes are constructed of UV-transparent acrylic with an open bottom to allow interaction with natural sediments (Fig. 5D). The 10 mm acrylic wall thickness has approximately a 20% loss of intensity across the whole PAR range up to 400 nm (near ultraviolet). Each flume is divided into three sections (Fig. 5C,D), with the outer sections used to house experimental organisms and the central section left empty for improved water velocity measurements and to determine the baseline physiological responses from the sediment biota. The experimental sections have guillotine-style sliding doors that allow the flume to be periodically sealed for respirometry and calcification measurements. Each of the doors has a silicone gasket and is secured with plastic screws to the flume lid. Pseudo-doors with silicone gasket seal the gap in the lid when the doors are not in use. Each of the three flume sections includes an outlet port with a leur-lock valve to accommodate carbonate chemistry sampling.

Experimental Design. From December 17–22 the CP-FOCE was deployed on the Heron Island reef flat for a short-term experiment. Three experimental flumes were deployed including a control flume, a flume with a pH offset of 0.06 pH and 0.22 pH units (Fig. 5A). pH projections for 2100 range from −0.14 to −0.35 depending on the emission scenario⁵⁰ and we chose −0.06 and −0.22 treatments as a conservative and middle of the road scenario, and were able to maintain these pH treatments as offsets from the dynamic ambient pH conditions.

In each of the three CP-FOCE flumes there was a plastic rack in one of the 3 compartments that contained 10, 8–10 cm long coral branches (*Acropora millepora*), one that contained 10, 3 cm diameter crustose coralline algae fragments (*Porolithon onkodes*), and a central flume containing only the natural reef sediments. The *A. millepora* and *P. onkodes* were collected by hammer and chisel on the Heron Island reef flat near the experimental area and allowed to recover for two week before being used in the experiments.

Carbonate Chemistry. Seven 50 ml syringes of seawater were sampled from each flume and the environment every four hours throughout the experiment and used to measure A_T , DIC, pH, and dissolved oxygen (Fig. 1). The syringe samples were immediately sealed upon collection and then transferred without contact to the atmosphere into sealed glass bottles. Incubations for photosynthesis and calcification rate estimations were performed each day: between 14:30–16:30 on Dec 18–20th, and between 12:30–14:30 on Dec 21st. All three flumes were closed for two hours using the guillotine doors and pumps inside the flumes turned on to provide water movement within the closed flumes. Seawater samples were taken just before the flumes were closed and before they were reopened and the change in A_T was used to determine calcification rates using the total A_T anomaly method³¹. The volume of the coral and algal samples were determined by the volume displacement method and used in calcification and photosynthesis rate calculations.

A_T in the water samples was determined with a Mettler Toledo T50 automated titrator (Mettler Toledo, Langacher, Switzerland) with a 1 ml burette, a small volume DGi101-SC pH sensor, and a small volume stirrer. Titrations were performed with 0.1 M HCl and replicate 20 g seawater samples using the Gran titration method in a two-stage, potentiometric, open-cell titration⁵¹, with precision of $\pm 3 \mu\text{mol} \times \text{kg}^{-1}$ or better. Acid concentration was calibrated at the beginning of each run using Certified Reference Materials (CRMs) from A.G. Dickson (SIO, Oceanic Carbon Dioxide Quality Control).

DIC was sampled into 30 ml glass vials after being filtered with a 0.45 μM syringe filter, fixed with 15 μL saturated mercuric chloride solution and then sealed with a rubber lid and aluminum cap (Wheaton, USA). DIC was measured by infrared adsorption via a LICOR7000 $\text{CO}_2/\text{H}_2\text{O}$ analyzer coupled with a custom-made sample delivery system built by Stanford University's Stable Isotope Laboratory. The precision of DIC analyses of this system is typically better than $2 \mu\text{mol} \times \text{kg}^{-1}$ based on duplicate and triplicate analyses of >4000 seawater samples analyzed with this system. Seawater CRMs were analyzed every 6 samples to ensure the accuracy of DIC was $\pm 1 \mu\text{mol} \times \text{kg}^{-1}$.

pH samples were measured with a Denver pH meter and combination electrode (UB-10, Denver Instrument, NY, USA). The electrode was calibrated with NBS scale standard buffers of 7.000 and 10.012 (Radiometer analytical, Lyon, France) and then soaked in seawater for one hour before measurements.

Dissolved oxygen values were determined using the modified Winkler method⁵³ on samples preserved in 50 ml BOD bottles using a Metrohm titrator. Results obtained from duplicate samples were all within the acceptable range of analytical error ($\pm 1 \text{ ml} \times \text{L}^{-1}$).

Measured A_T , DIC, and T along with average Heron reef flat salinity of 34.7 psu were used to derive other carbonate system parameters (pCO_2 , CO_3^{2-} , Ω_{arag}) using CO_2SYS ⁵⁴. Dissociation constants K1 and K2 were calculated according to Merzbach et al. (1973)⁵⁵ refit by Dickson and Millero (1987)⁵⁶, and KSO_4 was from Dickson (1990)⁵⁷.

Dissolution Experiments. To obtain an estimate of Mg-calcite dissolution rates, samples of dead CCA's were placed in the control and each of the treatment flumes. These samples were collected fresh and sun dried for several days until there was no measurable photosynthetic activity, as measured by pulse amplitude modulated fluorometer (PAM, Waltz, Germany). At the beginning and end of the experiment, samples were oven dried at 40 °C and weighed to the nearest 0.00001 g. The mol% MgCO_3 of the individual CCA samples was measured using X-ray Diffraction (XRD), following Nash 2011⁴⁶. Carbonate mineral phases were quantified by XRD using the area under the curve method⁵⁸ and bulk magnesium was measured by inductively coupled plasma atomic emission spectroscopy (ICP-AES) on a subset of four of the samples that had the highest and lowest weight loss⁴⁶.

Statistics. All tests for statistically significant difference between populations were performed with single factor, one-way ANOVAs.

Data Management. Data used in the analyses for this paper have been deposited with the NOAA National Oceanographic Data Center (NODC). Please contact NODC directly to obtain a copy of these data.

- Raupach, M. R. et al. Global and regional drivers of accelerating CO_2 emissions. *Proc Natl Acad Sci USA* **104**, 10288–10293 (2007).
- Sabine, C. L. et al. The oceanic sink for anthropogenic CO_2 . *Science* **305**, 367–371 (2004).
- Pagani, M., Liu, Z. H., LaRiviere, J. & Ravelo, A. C. High Earth-system climate sensitivity determined from Pliocene carbon dioxide concentrations. *Nat Geosci* **3**, 27–30 (2010).
- Hönisch, B. et al. The geological record of ocean acidification. *Science* **335**, 1058–1063 (2012).
- Millero, F. J. The marine inorganic carbon cycle. *Chem Rev* **107**, 308–341 (2007).
- Caldeira, K. & Wickett, M. E. Anthropogenic carbon and ocean pH. *Nature* **425**, 365–366 (2003).
- Feely, R. A. et al. Impact of anthropogenic CO_2 on the CaCO_3 system in the oceans. *Science* **305**, 362–366 (2004).
- Pelejero, C., Calvo, E. & Hoegh-Guldberg, O. Paleo-perspectives on ocean acidification. *Trends Ecol Evol* **25**, 332–344 (2010).
- Caldeira, K. & Wickett, M. E. Ocean model predictions of chemistry changes from carbon dioxide emissions to the atmosphere and ocean. *J Geophys Res-Oceans* **110**, C09S04 (2005).
- Solomon, S. Intergovernmental Panel on Climate Change. Working Group I. Climate change 2007: the physical science basis: contribution of Working Group I to the Fourth Assessment Report of the Intergovernmental Panel on Climate Change. (Cambridge University Press, 2007).
- Doney, S. C., Fabry, V. J., Feely, R. A. & Kleypas, J. A. Ocean acidification: the other CO_2 problem. *Annu Rev Mar Sci* **1**, 169–192 (2009).
- Kleypas, J. A. & Yates, K. K. Coral reefs and ocean acidification. *Oceanography* **22**, 108–117 (2009).
- Schneider, K. & Erez, J. The effect of carbonate chemistry on calcification and photosynthesis in the hermatypic coral *Acropora eurystoma*. *Limnol Oceanogr* **51**, 1284–1293 (2006).
- Hendriks, I. E., Duarte, C. M. & Alvarez, M. Vulnerability of marine biodiversity to ocean acidification: A meta-analysis. *Estuar Coast Shelf Sci* **86**, 157–164 (2010).
- Dupont, S., Dorey, N. & Thorndyke, M. What meta-analysis can tell us about vulnerability of marine biodiversity to ocean acidification? *Estuar Coast Shelf Sci* **89**, 182–185 (2010).
- Anthony, K. R. N., Kline, D. I., Diaz-Pulido, G., Dove, S. & Hoegh-Guldberg, O. Ocean acidification causes bleaching and productivity loss in coral reef builders. *Proc Natl Acad Sci USA* **105**, 17442–17446 (2008).
- Morse, J. W., Arvidson, R. S. & Luttge, A. Calcium carbonate formation and dissolution. *Chem Rev* **107**, 342–381 (2007).
- Brewer, P. G. & Peltzer, E. T. Limits to marine life. *Science* **324**, 347–348 (2009).
- De'ath, G., Lough, J. M. & Fabricius, K. E. Declining coral calcification on the great barrier reef. *Science* **323**, 116–119 (2009).
- Cooper, T. F., De'ath, G., Fabricius, K. E. & Lough, J. M. Declining coral calcification in massive Porites in two nearshore regions of the northern Great Barrier Reef. *Glob Change Biol* **14**, 529–538 (2008).
- Carpenter, K. E. et al. One-third of reef-building corals face elevated extinction risk from climate change and local impacts. *Science* **321**, 560–563 (2008).
- Hofmann, G. E. et al. High-frequency dynamics of ocean pH: a multi-ecosystem comparison. *PLoS One* **6**, e28983 (2011).
- Shaw, E. C., McNeil, B. I. & Tilbrook, B. Impacts of ocean acidification in naturally variable coral reef flat ecosystems. *J Geophys Res-Oceans* **117**, C03038 (2012).



24. Gagliano, M., McCormick, M., Moore, J. & Depczynski, M. The basics of acidification: baseline variability of pH on Australian coral reefs. *Mar Biol* **157**, 1849–1856 (2010).
25. Santos, I. R., Glud, R. N., Maher, D. & Eyre, B. D. Diel coral reef acidification driven by pore water advection in permeable carbonate sands, Heron Island, Great Barrier Reef. *Geophys Res Lett* **38**, L03604 (2011).
26. Fabricius, K. E. *et al.* Losers and winners in coral reefs acclimatized to elevated carbon dioxide concentrations. *Nat Clim Change* **1**, 165–169 (2011).
27. Barry, J. P. From extreme CO₂ venting to ocean acidification - Experimental approaches to assess the fate of deep sea ecosystems. *Geochim Cosmochim Acta* **73**, A93–A93 (2009).
28. Hall-Spencer, J. M. *et al.* Volcanic carbon dioxide vents show ecosystem effects of ocean acidification. *Nature* **454**, 96–99 (2008).
29. Munro, D. R., Dunbar, R. B., Mucciarone, D. A. & Arrigo, K. R. Stable isotope composition of dissolved inorganic carbon and particulate organic carbon in sea ice from the Ross Sea, Antarctica. *J Geophys Res* **115**, 14 (2010).
30. Manzello, D. P. *et al.* Poorly cemented coral reefs of the eastern tropical Pacific: Possible insights into reef development in a high-CO₂ world. *Proc Nat Acad Sci Usa* **105**, 10450–10455 (2008).
31. Guinotte, J. M. *et al.* Will human-induced changes in seawater chemistry alter the distribution of deep-sea scleractinian corals? *Front Ecol Environ* **4**, 141–146 (2006).
32. Turley, C. M., Roberts, J. M. & Guinotte, J. M. Corals in deep-water: will the unseen hand of ocean acidification destroy cold-water ecosystems? *Coral reefs* **26**, 445–448 (2007).
33. Kleypas, J. A. *et al.* Geochemical consequences of increased atmospheric carbon dioxide on coral reefs. *Science* **284**, 118–120 (1999).
34. Yates, K. K. & Halley, R. B. Measuring coral reef community metabolism using new benthic chamber technology. *Coral reefs* **22**, 247–255 (2003).
35. Yates, K. K. & Halley, R. B. CO₃²⁻ concentration and pCO₂ thresholds for calcification and dissolution on the Molokai reef flat, Hawaii. *Biogeosciences* **3**, 357–369 (2006).
36. Silverman, J., Lazar, B. & Erez, J. Effect of aragonite saturation, temperature, and nutrients on the community calcification rate of a coral reef. *J Geophys Res-Oceans* **112**, C05004 (2007).
37. Silverman, J., Lazar, B., Cao, L., Caldeira, K. & Erez, J. Coral reefs may start dissolving when atmospheric CO₂ doubles. *Geophys Res Lett* **36**, L05606 (2009).
38. Form, A. U. & Riebesell, U. Acclimation to ocean acidification during long-term CO₂ exposure in the cold-water coral *Lophelia pertusa*. *Glob Change Biol* **18**, 843–853 (2012).
39. McCulloch, M., Falter, J., Trotter, J. & Montagna, P. Coral resilience to ocean acidification and global warming through pH up-regulation. *Nat Clim Change*, In press (2012).
40. McCulloch, M. *et al.* Resilience of cold-water scleractinian corals to ocean acidification: Boron isotopic systematics of pH and saturation state up-regulation. *Geochimica et Cosmochimica Acta*, In press (2012).
41. Barry, J., Hall-Spencer, J. & Tyrrell, T. in *Guide to best practices for ocean acidification research and data reporting* (eds Riebesell, U., Fabry, V. J., Hansson, L. & Gattuso, J. P.) 123–136 (Publications Office of the European Union, 2010).
42. Walz, P. M., Kirkwood, W. J., Peltzer, E. T., Hester, K. C. & Brewer, P. G. Creating controlled CO₂ perturbation experiments on the seafloor - Development of FOCE techniques. *Oceans 2008 - Mts/leee Kobe Techno-Ocean, Vols 1–3*, 750–753 (2008).
43. Dunbar, R. B., Mucciarone, D. A., Long, M. & Sohst, B. Hydrographic properties of the ross sea continental shelf during November-December, 2006. *NBP0608 - CORSACS II, Stanford University Ocean Biogeochemistry Group, Report 07-0*, 23 (2007).
44. Santos, I. R., Glud, R. N., Maher, D., Erler, D. & Eyre, B. D. Diel coral reef acidification driven by porewater advection in permeable carbonate sands, Heron Island, Great Barrier Reef. *Geophys Res Lett* **38**, L03604 (2011).
45. Andersson, A. J., Mackenzie, F. T. & Bates, N. R. Life on the margin: implications of ocean acidification on Mg-calcite, high latitude and cold-water marine calcifiers. *Mar Ecol-Progr Ser* **373**, 265–273 (2008).
46. Nash, M. C. *et al.* First discovery of dolomite and magnesite in living coralline algae and its geobiological implications. *Biogeosciences* **8**, 3331–3340 (2011).
47. Melzner, F. *et al.* Future ocean acidification will be amplified by hypoxia in coastal habitats. *Marine Biol, In Press* (2012).
48. Tribollet, A., Godinot, C., Atkinson, M. & Langdon, C. Effects of elevated pCO₂ on dissolution of coral carbonates by microbial euendoliths. *Global Biogeochem Cycles* **23**, GB3008 (2009).
49. Oriordan, C. A., Monismith, S. G. & Koseff, J. R. A Study of Concentration Boundary-Layer Formation over a Bed of Model Bivalves. *Limnol Oceanogr* **38**, 1712–1729 (1993).
50. Randall, D. A. *et al.* in *Climate Change 2007: The Physical Science Basis. Contribution of Working Group 1 to the Fourth Assessment Report of the Intergovernmental Panel on Climate Change* (eds Solomon, S. D. *et al.*) (Cambridge University Press, 2007).
51. Marker, M. *et al.* The Coral Proto Free Ocean Carbon Enrichment System (CP-FOCE): Engineering and Development. *OCEANS IEEE* **2010**, 1–10 (2010).
52. Dickson, A. G., Afghan, J. D. & Anderson, G. C. Reference materials for oceanic CO₂ analysis: a method for the certification of total alkalinity. *Mar Chem* **80**, 185–197 (2003).
53. Strickland, J. D. H. & Parsons, T. R. A practical handbook of seawater analysis. *Bull Fish Res Bd Canada, Bull* **167**, 311 p. (1972).
54. Lewis, E. & Wallace, W. R. CO₂SYS-Program developed for the CO₂ system calculations. (Carbon Dioxide Information Analysis Center, Oak Ridge, Tennessee, 1998).
55. Mehrbach, C., Culbertson, C. H., Hawley, J. E. & Pytkowicz, R. M. Measurement of the apparent dissociation constants of carbonic acid in seawater at atmospheric pressure. *Limnol Oceanogr* **18**, 897–907 (1973).
56. Dickson, A. G. & Millero, F. J. A comparison of the equilibrium constants for the dissociation of carbonic acid in seawater media. *Deep Sea Res* **34**, 1733–1743 (1987).
57. Dickson, A. G. Standard potential of the reaction: AgCl(s) + 1/2 H₂(g) = Ag(s) + HCl(aq), and the standard acidity constant of the ion HSO⁻⁴ in synthetic seawater from 273.15 to 318.15 K. *J Chem Thermodyn* **22**, 113–127 (1990).
58. Sepulcre, S., Durand, N. & Bard, E. Mineralogical determination of reef and periplatform carbonates: Calibration and implications for paleoceanography and radiochronology. *Global Planet Change* **66**, 1–9 (2009).
59. Ricker, W. E. Linear regressions in fishery research. *Bull Fish Res Bd Canada, Bull* **30**, 409–434 (1973).
60. Kuffner, I. B., Andersson, A. J., Jokiel, P. L., Rodgers, K. S. & Mackenzie, F. T. Decreased abundance of crustose coralline algae due to ocean acidification. *Nat Geosci* **1**, 114–117 (2008).

Acknowledgments

The authors wish to acknowledge the Australian Research Council (ARC) Linkage Infrastructure, Equipment and Facilities grant #LE0989608, ARC Linkage grant #LP0775303, ARC Centre of Excellence grant #CE0561435, a Queensland Government Smart State Premier's Fellowship to OHG, National Science Foundation grants (NSF OCE-0729236, to RBD and JRK; and NSF ATM-0941760 to BGM), and the Pacific Blue Foundation for supporting this research. We also wish to thank the staff of the Heron Island Research station especially Matt Roy, Steve Venn, Kyra Hay, and Liz Perkins for all of their support throughout this project. Permits from the Department of Environment and Resource Management (#CSCE00874010) and the Great Barrier Reef Marine Park Authority (#G09/29996.1) were provided to conduct this research.

Author Contributions

DIK, LT, and KS wrote the main manuscript text, DIK, LT, and MN prepared the figures, MN and BO did the XRD and ICP measurements, DIK, LT, KS, TM, AC, MM, KH, BO, MN, MV, JC, BDR, SDC, SD and OHG participated in field work and carbonate chemistry measurements. All authors reviewed the manuscript.

Additional information

Competing financial interests: The authors declare no competing financial interests.

License: This work is licensed under a Creative Commons Attribution-NonCommercial-ShareAlike 3.0 Unported License. To view a copy of this license, visit <http://creativecommons.org/licenses/by-nc-sa/3.0/>

How to cite this article: Kline, D.I. *et al.* A short-term *in situ* CO₂ enrichment experiment on Heron Island (GBR). *Sci. Rep.* **2**, 413; DOI:10.1038/srep00413 (2012).